Journal of Physics: Conference Series

On the sensitivity of positron annihilation signals to alloy homogeneity in $In_xGa_{1-x}N$

To cite this article: F Tuomisto *et al* 2014 *J. Phys.: Conf. Ser.* **505** 012042

Journal of Physics: Conference Series **505** (2014) 012042 doi:10.1088/1742-6596/505/1/012042

On the sensitivity of positron annihilation signals to alloy homogeneity in $In_xGa_{1-x}N$

F Tuomisto[1], **V Norrman**[1] **and I Makkonen**[2]
[1] Department of Applied Physics, Aalto University, POB 11100, 00076 Aalto, Finland
[2] COMP Centre of Excellence, Helsinki Institute of Physics and Department of Applied Physics, Aalto University, POB 11100, 00076 Aalto, Finland

E-mail: filip.tuomisto@aalto.fi

Abstract. We present results of theoretical calculations of positron annihilation signals in InGaN alloys with and without vacancies. We demonstrate the sensitivity of the signals to the different configurations of the In/Ga atoms in $In_{1-x}Ga_xN$ supercells.

1. Introduction

The two most used methods in defect studies with positron annihilation are the positron lifetime and Doppler broadening (of the positron-electron annihilation radiation) spectroscopy [1]. These techniques are very efficient in giving important information on vacancy defects in metals and semiconductors: vacancies can be identified (sublattice in compounds, size in the case of vacancy clusters, and decoration by impurities), their charge states can be determined and their concentrations can be evaluated in the technologically important range from 10^{15} to 10^{19} cm^{-3}. Thanks to recent developments in theoretical calculations, computational studies can be directly compared with positron experiments providing possibilities for very detailed interpretations of experimental data [2–6].

The identification of a vacancy defect is at its best when the host lattice has perfect crystalline order. Good examples of such cases include the vacancy-donor complexes in Si [7–10], the Ga and As vacancies in GaAs [11–14], or the Ga vacancy-impurity complexes in GaN [15–18]. In some cases even small substitutional impurities can act as vacancy defects and be identified, such as Li_{Zn} in ZnO [19,20]. As positron trapping to negative defects is temperature dependent, manipulation of the defect charge states through optical illumination can be used to bring additional detail to the identification, as in the case of the EL2 defect in GaAs [21,22] or vacancy clusters in diamond [23–25].

Many of the technologically important semiconductors are in fact alloys instead of simple elemental or compound systems. Detailed identification of vacancy defects has been possible for example in $Si_{1-x}Ge_x$: vacancy-fluorine [26,27] and vacancy-donor [28–30] complexes have been studied quite extensively. However, the random nature of the alloy brings additional complication to the analysis, as the immediate vicinity of the vacancy defect is not well defined. For example, the three group IV atoms surrounding the vacancy in the *V*-Sb complex in $Si_{1-x}Ge_x$ can all be Ge (or all Si). As the core electron shells of Ge and Si are very different, the effect on the annihilation signals is strong.

The main advantage of the III-nitride family of compounds (AlN, GaN and InN) is the possibility to synthesize alloys in order to tune the optical properties (band gap) for the fabrication of opto-electronic devices. Hence it is important to understand the physics of defects in these alloys. In addition, the alloying seems to generate material with elevated point (vacancy) defect concentrations

[31–33]. However, the random alloy nature makes the detailed identification of the detected defects very difficult [34,35], even if it is possible in the respective binary compounds [36–40].

In this paper we present results of theoretical calculations of positron annihilation signals in InGaN systems with and without vacancies. We demonstrate the sensitivity of the signals to the different configurations of the In/Ga atoms. We discuss these results in the light of published experimental data in thin film InGaN alloys and other alloyed materials systems. We also present our view on future developments required for more detailed analysis of defects in semiconductors with less perfect crystalline order.

2. Methods

Our computational scheme [4] is based on the zero-positron density limit of the two-component density functional theory [41]. Valence electron densities are calculated self-consistently using the local density approximation (LDA) and projector augmented-wave method (PAW) [42] implemented in the VASP code [43]. The electronic structure calculations for bulk systems are performed using a 16-atom InGaN wurtzite supercell, with 34 different ways of distributing the In and Ga atoms in the cell. For systems containing a vacancy the supercell size was increased to 128 atoms by multiplying the original 16-atom cell. Ionic positions are relaxed with a convergence criterion of 0.01 eV/Å for forces. Gallium 3*d* and indium 4*d* electrons are included as valence electrons and an energy cutoff of 400 eV is chosen. The Brillouin zone is sampled with a 4×4×4 Monkhorst-Pack **k**-point mesh. After deriving the electron densities in the lattice, the positron densities are solved independently in the calculated Coulomb potential due to electrons and nuclei and the *e-p* correlation potential evaluated with in LDA [41]. This is the so-called "conventional scheme", in which the positron does not affect the average electron density, and further, the *e-p* correlation potential is approximated in the zero-positron-density limit. Momentum densities of annihilating electron-positron pairs are calculated using the state-dependent enhancement model [44] within LDA.

In order to compare the calculated three-dimensional (3D) momentum density to one-dimensional (1D) experimental spectra, we integrate the calculated spectra over the wurtzite *m* plane. To account for the experimental detector resolution, the calculated momentum distributions are additionally convoluted with a Gaussian resolution function of 0.66 a.u. FWHM The line-shape parameters are calculated from the spectra using momentum windows $S < 0.40$ a.u. and $1.53 < W < 3.93$ a.u. The positron lifetime τ is determined as the inverse of the annihilation rate λ obtained from the calculations. For further details on the computational methods, the reader is referred to [3,4,38].

3. Results and discussion

3.1. Bulk InGaN systems

Figures 1–3 show the *S* and *W* parameters and the positron lifetimes calculated in 16-atom InGaN supercells with varying In content and In-Ga distributions. Interestingly, the *S* and *W* parameters (figures 1 and 2) change in different ways with increasing In content. The change in *W* parameter is very close to linear, while the S parameter exhibits strong bowing. The dotted curves are drawn to guide the eye, but also represent a simple model where positrons are considered to be attracted to GaN-resembling and InN-resembling lattices in different ways. For example, in figure 1 the dotted curve is drawn assuming that the relative weights of GaN and InN S parameters are 64% and 36%, respectively. Hence it would seem that from the *S* parameter point of view, positrons are almost twice as likely to annihilate in the GaN-resembling part than in the InN-resembling part of the InGaN lattice. On the other hand, the *W* parameters and the positron lifetimes do not exhibit any significant bowing (or preference), here the relative weights can be modelled as 53% and 47% for GaN and InN, respectively. The bowing seen in figure 4 hence fully originates from the *S* parameter bowing.

Both the S and W parameters for a given In content exhibit scatter as a function of the In-Ga distribution in the supercell, and the largest variations are seen for $In_{0.5}Ga_{0.5}N$. The variations are much smaller in the positron lifetime (figure 3). Interestingly, also the largest variations in *S* and *W* follow the simple model (dotted curve in figure 4), even if they cross the linear behaviour in figures 1 and 2.

The largest variations in the $In_{0.375}Ga_{0.625}N$ – $In_{0.625}Ga_{0.375}N$ supercells (points clearly separated from the others) are due to effective superlattice structure produced by the supercell.

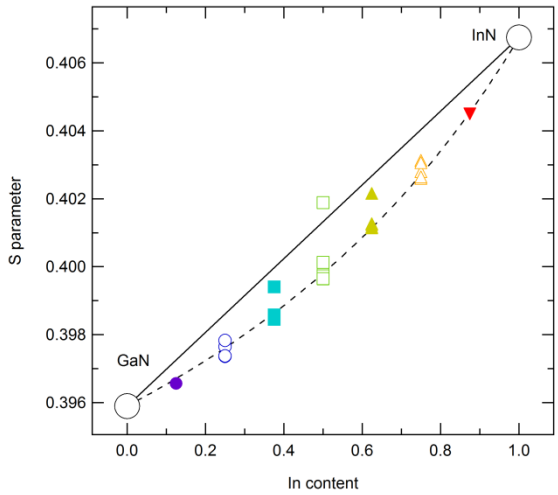

Figure 1. *S* parameters for $In_xGa_{1-x}N$ supercells with varying In-Ga distributions as a function of In content.

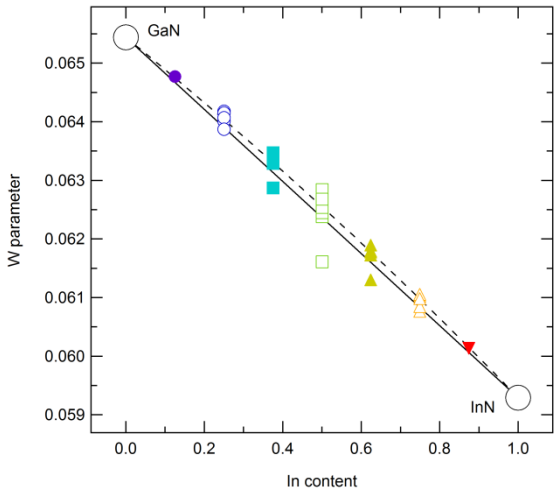

Figure 2. *W* parameters for $In_xGa_{1-x}N$ supercells with varying In-Ga distributions as a function of In content.

It is important to note that the above calculated positron annihilation parameters are not directly comparable on the absolute scale to experimental values. For example, the bulk positron lifetimes for both InN and GaN are 25–30 ps shorter than those determined experimentally. This is in line with earlier comparisons when the LDA approximation is employed [17,34,38]. The relative changes in the positron lifetime can, however, be considered reliable as found in these reports. The situation with the *S* and *W* parameters is more complex. In experiments we have $S_{InN} / S_{GaN} \approx 1.045$ [36], while in the calculations the ratio is 1.028. For the *W* parameter experiments give $W_{InN} / W_{GaN} \approx 0.86$, and the calculated ratio is 0.89. Interestingly, the experiments and theory are closer matched for the *W* parameter.

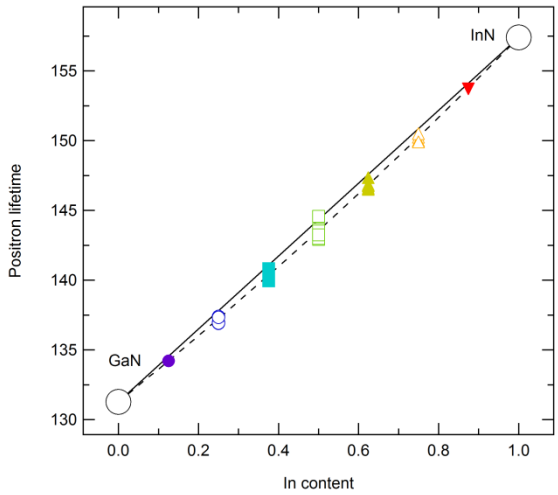

Figure 3. Positron lifetimes for $In_xGa_{1-x}N$ supercells with varying In-Ga distributions as a function of In content.

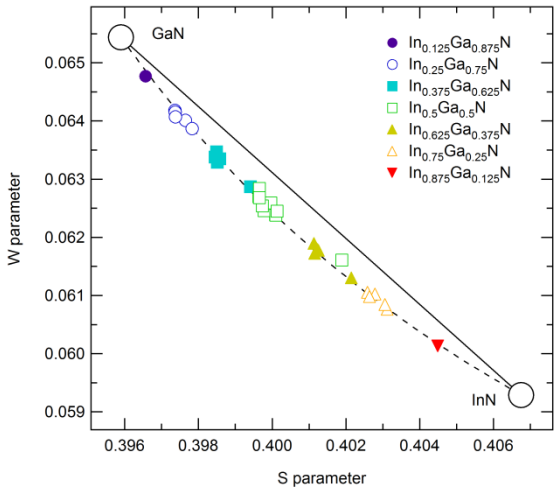

Figure 4. *S* and *W* parameters for $In_xGa_{1-x}N$ supercells with varying In-Ga distributions as a function of In content.

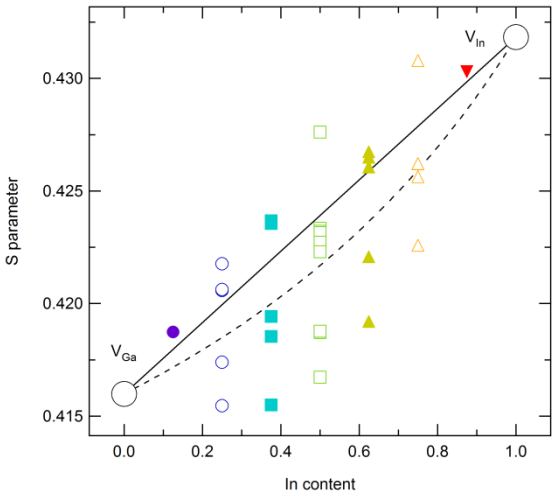

Figure 5. *S* parameters for metal vacancy containting $In_xGa_{1-x}N$ supercells with varying In-Ga distributions as a function of In content.

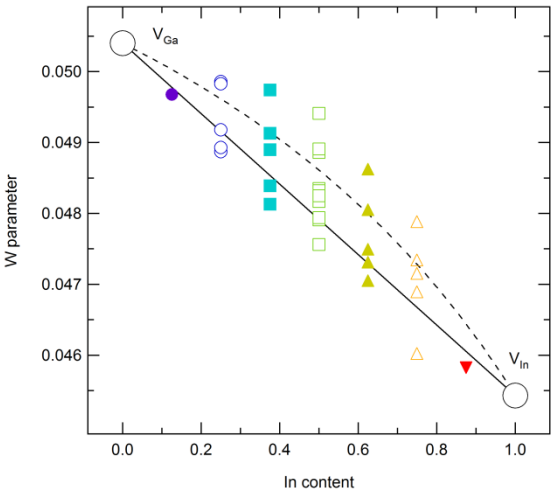

Figure 6. *W* parameters for metal vacancy containting $In_xGa_{1-x}N$ supercells with varying In-Ga distributions as a function of In content.

3.2. Vacancy-containing InGaN systems

Figures 5–7 show the S and W parameters and the positron lifetimes calculated in 128-atom InGaN supercells containing one metal vacancy with varying In content and In-Ga distributions. The removed metal atom was chosen at random in the cell, and only one vacancy for each of the 34 above-descibred systems was considered. Agreement with experiment is similar as in the case of bulk systems.

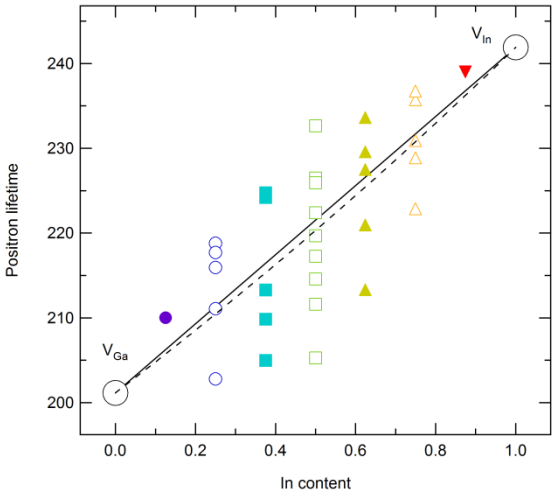

Figure 7. Positron lifetimes for metal vacancy containting $In_xGa_{1-x}N$ supercells with varying In-Ga distributions as a function of In content.

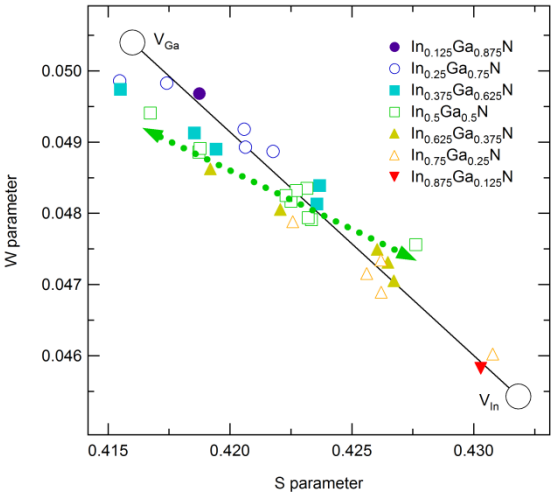

Figure 8. *S* and *W* parameters for metal vacancy containting $In_xGa_{1-x}N$ supercells with varying In-Ga distributions as a function of In content.

The dotted lines in the figures represent a similar model as for the bulk (relative weights for V_{Ga} and V_{In} are 64% and 36%, respectively, in figures 5 and 6), but as the scatter is much more important than in the bulk supercells, the main observation that should be made is that the points are clearly below the linear behaviour in figure 5 and above in figure 6. The scatter is very large also for the calculated positron lifetimes, covering 70% of the total difference between V_{Ga} and V_{In} for the $In_{0.5}Ga_{0.5}N$ supercell (figure 7). Interestingly, as seen in figure 8, the S and W parameters do not deviate strongly from the V_{Ga}-V_{In} line, even if the strong scatter (shown by the green arrow

$In_{0.5}Ga_{0.5}N$) is evident. The number of Ga/In atoms in the 12-atom next-neighbor shell surrounding the metal vacancy has a strong influence on the annihilation parameters too, but detailed correlation of these effects requires further studies.

3.3. Notes and comparison to other alloys

An important observation is that the above considerations suggest that it is very difficult to distinguish the effects of low vacancy concentrations from alloy homogeneity effects in conventional Doppler broadening experiments in $In_{1-x}Ga_xN$ materials. Experimental investigations also in elemental semiconductor alloys, namely $Si_{1-x}Ge_x$, have suggested similar interpretations [28-30]: after introducing vacancy defects by irradiation and then removing them by annealing, the lattice Si/Ge distribution changes in such a way that the *S* and *W* parameters are different from the original situation. Further investigations, both theoretical and experimental, are necessary in order to elucidate whether positron annihilation methods could be used to assess, e.g., In clustering in $In_{1-x}Ga_xN$ in a similar manner as in metal alloys [45].

4. Summary

We have performed preliminary theoretical calculations of positron annihilation signals in InGaN supercelles with and without metal vacancies. Our results demonstrate the strong sensitivy of the Doppler broadening S and W parameters as well as of the positron lifetime to the alloy (dis)order in $In_{1-x}Ga_xN$. Related observations can be made in other alloyed semiconductors such as $Si_{1-x}G_xe$.

Acknowledgment

This work was partially funded by the Academy of Finland.

References

[1] Tuomisto F and Makkonen 2013 I *Rev. Mod. Phys.* **85** 1583
[2] Ishibashi S 2004 *Mater. Sci. Forum* **445-446** 401
[3] Makkonen I, Hakala M and Puska M J 2005 *J. Phys. Chem. Solids* **66** 1128
[4] Makkonen I, Hakala M and Puska M J 2006 *Phys. Rev. B* **73** 03513
[5] Ishibashi S, Tamura T, Tanaka S, Kohyama M and Terakura K 2007 *Phys. Rev. B* **76** 153310
[6] Wiktor J, Jomard G, Torrent M and Bertolus M 2013 *Phys. Rev. B* **87** 235207
[7] Lawther D W, Myler U, Simpson P J, Rousseau P M, Griffin P B and Plummer J D 1995 *Appl. Phys. Lett.* **67** 3575
[8] Saarinen K, Nissilä J, Kauppinen H, Hakala M, Puska M J, Hautojärvi P and Corbel C 1999 *Phys. Rev. Lett.* **82** 1883
[9] Ranki V, Pelli A and Saarinen K 2004 *Phys. Rev. B* **69** 115205
[10] Rummukainen M, Makkonen I, Ranki V, Puska M J, Saarinen K and Gossmann H-J L 2005 *Phys. Rev. Lett.* **94** 165501
[11] LeBerre C, Corbel C, Brozel M R, Kuisma S, Saarinen K and Hautojärvi P 1994 *J. Phys.: Condens. Matter* **6** L759
[12] Le Berre C, Corbel C, Saarinen K, Kuisma S, Hautojärvi P and Fornari R 1995 *Phys. Rev. B* **52** 8112
[13] Kuisma S, Saarinen K, Hautojärvi P, Corbel C and LeBerre C 1996 *Phys. Rev. B* **53** 9814
[14] Gebauer J, Lausmann M, Staab T E M, Krause-Rehberg R, Hakala M and Puska M J 1999 *Phys. Rev. B* **60** 1464
[15] Saarinen K, Laine T, Kuisma S, Nissilä J, Hautojärvi P, Dobrzynski L, Baranowski J M, Pakula K P, Stepniewski R, Wojdak M, Wysmolek A, Suski T, Leszczynski M, Grzegory I and Porowski S 1997 *Phys. Rev. Lett.* **79** 3030
[16] Hautakangas S, Oila J, Alatalo M, Saarinen K, Liskay L, Seghier D and Gislason H P 2003 *Phys. Rev. Lett.* **90** 137402

[17] Hautakangas S, Makkonen I, Ranki V, Puska M J, Saarinen K, Xu X and Look D C 2006 *Phys. Rev. B* **73** 193301
[18] Nykänen H, Suihkonen S, Kilanski L, Sopanen M and Tuomisto F 2012 *Appl. Phys. Lett.* **100** 122105
[19] Johansen K M, Zubiaga A, Makkonen I, Tuomisto F, Neuvonen P T, Knutsen K E, Monakhov E V, Kuznetsov A Yu and Svensson B G 2011 *Phys. Rev. B* **83** 245208
[20] Johansen K M, Zubiaga A, Tuomisto F, Monakhov E V, Kuznetsov A Yu and Svensson B G 2011 *Phys. Rev. B* **84** 115203
[21] Krause R, Saarinen K, Hautojärvi P, Polity A, Gärtner G and Corbel C 1990 *Phys. Rev. Lett.* **65** 3329
[22] Saarinen K, Kuisma S, Hautojärvi P, Corbel C and LeBerre C 1994 *Phys. Rev. B* **49** 8005
[23] Dannefaer S, Pu A and Kerr K 2001 *Diamond Rel. Mater.* **10** 2113
[24] Mäki J-M, Tuomisto F, Varpula A, Fisher D, Khan R U A and Martineau P M 2011 *Phys. Rev. Lett.* **107** 217403
[25] Mäki J-M, Kuittinen T, Korhonen E and Tuomisto F 2012 *New J. Phys.* **14** 035023
[26] Pi X D, Burrows C P and Coleman P G 2003 *Phys. Rev. Lett.* **90** 155901
[27] Edwardson C J, Coleman P G, Mubarek H A W E and Gandy A S 2012 *J. Appl. Phys.* **111** 073510
[28] Kuitunen K, Tuomisto F and Slotte J 2007 *Phys. Rev. B* **76** 233202
[29] Kilpeläinen S, Kuitunen K, Tuomisto F, Slotte J, Radamson H H and Kuznetsov A Yu 2010 *Phys. Rev. B* **81** 132103
[30] Kilpeläinen S, Tuomisto F, Slotte J, Lundsgaard Hansen J and Nylandsted Larsen A 2011 *Phys. Rev. B* **83** 094115
[31] Onuma T, Chichibu S F, Uedono A, Sota T, Cantu P, Katona T M, Keading J F, Keller S, Mishra U K, Nakamura S and DenBaars S P 2004 *J. Appl. Phys.* **95** 2495
[32] Slotte J, Tuomisto F, Saarinen K, Moe C G, Keller S DenBaars S P 2007 *Appl. Phys. Lett.* **90** 151908
[33] Uedono A, Tenjinbayashi K, Tsutsui T, Shimahara Y, Miyake H, Hiramatsu K, Oshima N, Suzuki R and Ishibashi S 2012 *J. Appl. Phys.* **111** 013512
[34] Uedono A, Ishibashi S, Watanabe T, Wang X Q, Liu S T, Chen G, Sang L W, Sumiya M and Shen B 2012 *J. Appl. Phys.* **112** 014507
[35] Uedono A, Tsutsui T, Watanabe T, Kimura S, Zhang Y, Lozac'h M, Sang L W, Ishibashi S and Sumiya M 2013 *J. Appl. Phys.* **113** 123502
[36] Tuomisto F, Pelli A, Yu K M, Walukiewicz W and Schaff W J 2007 *Phys. Rev. B* **75** 193201
[37] Tuomisto F, Ranki V, Look D C and Farlow G C 2007 *Phys. Rev. B* **76** 165207
[38] Rauch C, Makkonen I and Tuomisto F 2011 *Phys. Rev. B* **84** 125201
[39] Mäki J-M, Makkonen I, Tuomisto F, Karjalainen A, Suihkonen S, Räisänen J, Chemekova T Yu and Makarov Yu N 2011 *Phys. Rev. B* **84** 081204
[40] Rauch C, Tuomisto F, King P D C, Veal T D, Lu H and Schaff W J 2012 *Appl. Phys. Lett.* **101** 011903
[41] Boroński E and Nieminen R M 1986 *Phys. Rev. B* **34** 3820
[42] Blöchl P E 1994 *Phys. Rev. B* **50** 17953
[43] Kresse G and Furthmüller J 1996 *Phys. Rev. B* **54** 11169
[44] Alatalo M, Barbiellini B, Hakala M, Kauppinen H, Korhonen T, Puska M J, Saarinen K, Hautojärvi P and Nieminen R M 1996 *Phys. Rev. B* **54** 2397
[45] Nagai Y, Hasegawa M, Tang Z, Hempel A, Yubuta K, Shimamura T, Kawazoe Y, Kawai A and Kano F 2000 *Phys. Rev. B* **61** 6574